PNAS RESEARCH ARTICLE | PLANT BIOLOGY

Spatiotemporal bifurcation of HY5-mediated blue-light signaling regulates wood development during secondary growth

Hyeona Hwang[a], Yookyung Lim[a], Myung-Min Oh[b], Hyunmo Choi[c], Donghwan Shim[d], Young Hun Song[e], and Hyunwoo Cho[a,1]

Affiliations are included on p. 12.

Edited by Hongtao Liu, Chinese Academy of Sciences Center for Excellence in Molecular Plant Sciences, Institute of Plant Physiology and Ecology, Shanghai, China; received April 15, 2024; accepted October 21, 2024 by Editorial Board Member Joseph J. Kieber

Plants have evolved photoreceptors to optimize their development during primary growth, including germination, hypocotyl elongation, cotyledon opening, and root growth, allowing them to adapt to challenging light conditions. The light signaling transduction pathway during seedling establishment has been extensively studied, but little molecular evidence is available for light-regulated secondary growth, and how light regulates cambium-derived tissue production remains largely unexplored. Here, we show that CRYPTOCHROME (CRY)-dependent blue light signaling and the subsequent attenuation of ELONGATED HYPOCOTYL 5 (HY5) movement to hypocotyls are key inducers of xylem fiber differentiation in *Arabidopsis thaliana*. Using grafted chimeric plants and hypocotyl-specific transcriptome sequencing of light signaling mutants under controlled light conditions, we demonstrate that the perception of blue light by CRYs in shoots drives secondary cell wall (SCW) deposition at xylem fiber cells during the secondary growth of hypocotyls. We propose that HY5 is a blue light–responsive mobile protein that inhibits xylem fiber formation via direct transcriptional repression of *NAC SECONDARY WALL THICKENING PROMOTING 3* (*NST3*). CRYs retain HY5 in the nucleus, impede its long-distance transport from leaf to hypocotyl, and they initiate *NST3*-driven SCW gene expression, thereby triggering xylem fiber production. Our findings shed light on the long-range CRYs-HY5-NST3 signaling cascade that shapes xylem fiber development, highlighting the activity of HY5 as a transcriptional repressor during secondary growth.

xylem fiber | secondary cell wall | secondary growth | blue light signaling | HY5

Significance

Plants use light to generate the products of photosynthesis, which serves as materials for secondary cell wall (SCW) formation, an essential process for secondary growth. However, how light signaling mediates secondary growth, independently of photosynthesis, has been elusive. We demonstrate that blue light signaling acts as a trigger for wood formation, a process regulated by long-distance signaling from light perceived in the shoot. Blue light-CRYPTOCHROME (CRY) signaling impedes the long-distance movement of ELONGATED HYPOCOTYL 5 (HY5) by retaining it in the nucleus. Wood formation is triggered by the release from HY5-mediated repression of SCW synthesis. Our findings provide insight into how plants utilize light quality information for wood formation and offer promising strategies to foster carbon capture and storage into woody biomass.

Plants perceive environmental signals and integrate them into growth patterns and developmental decisions throughout their lifecycles. Sunlight is one of the most important environmental factors affecting plants, providing the raw energy needed for photosynthesis and leading to major developmental changes known as photomorphogenesis when etiolated seedlings first perceive light and undergo light-mediated development (1). The functional characterization of mutants with altered physiology when exposed to light or dark conditions during primary growth of *Arabidopsis* (*Arabidopsis thaliana*) seedlings has revealed key factors involved in sensing (photoreceptors) and transducing information about light quality and duration to modulate developmental plasticity (2–9). Photoreceptors are categorized according to the specific wavelengths they absorb and respond to phytochromes (phys) for red/far-red (R/FR) light; cryptochromes, phototropins, and ZEITLUPE family members for blue/ultraviolet A (UV-A) light; and UVB-RESISTANCE 8 (UVR8) for UV-B. Cryptochromes (CRYs) utilize flavin adenine dinucleotide oxidation to detect blue light and signal transduction via oligomerization and liquid–liquid phase separation to regulate diverse physiological response such as early seedling growth, circadian entrainment, and flowering time (10–12).

Photoactivated crys regulate blue light responses via core transcriptional regulators together with phytohormones and downstream transcription factors such as CRYPTOCHROME-INTERACTING BASIC-HELIX-LOOP-HELIX proteins (CIBs), PHYTOCHROME-INTERACTING-FACTORs (PIFs), ELONGATED HYPOCOTYL 5 (HY5). Most light signaling eventually converges onto the common central regulator, the CONSTITUTIVE PHOTOMORPHOGENIC 1 (COP1)-SUPPRESSOR OF PHYA-105 (SPA) E3 ubiquitin ligase complex (13). Activation of light signaling via phys and CRYs inactivates the COP1–SPA complex, leading to the accumulation and stabilization of positive regulators of light-mediated development such as the basic leucine zipper (bZIP) transcription factor HY5 (14). HY5, a central regulator of photomorphogenesis, regulates a wide range of developmental processes such as hypocotyl elongation, chloroplast development, primary root growth, lateral root development, anthocyanin biosynthesis, and nutrient uptake in response

Author contributions: H. Cho designed research; H.H. and Y.L. performed research; M.-M.O., H. Choi, D.S., and Y.H.S. contributed new reagents/analytic tools; H.H. and H. Cho analyzed data; and H.H. and H. Cho wrote the paper.

The authors declare no competing interest.

This article is a PNAS Direct Submission. H.L. is a guest editor invited by the Editorial Board.

Copyright © 2024 the Author(s). Published by PNAS. This article is distributed under Creative Commons Attribution-NonCommercial-NoDerivatives License 4.0 (CC BY-NC-ND).

[1]To whom correspondence may be addressed. Email: hwcho@chungbuk.ac.kr.

This article contains supporting information online at https://www.pnas.org/lookup/suppl/doi:10.1073/pnas.2407524121/-/DCSupplemental.

Published November 25, 2024.

to light (15–17). HY5 is an atypical bZIP transcription factor lacking a transcriptional activation or repression domain, which are required by cotranscriptional regulators to control the activities of numerous ACGT motif-containing promoters (18). Besides the local effect of HY5 as a transcriptional regulator inside the nucleus, its shoot-to-root mobility also serves as an important signaling cue for integrating information about light conditions to belowground tissue for development (19–25). Despite the comprehensive characterization of the photoreceptor-mediated regulation of HY5 activity in many environmental and developmental contexts, how HY5-centered light signaling output is bifurcated across developmental stages and how it acts locally or systematically during light-mediated development are largely unknown.

During the evolution of land plants, competition for light resulted in the development of adaptive strategies to grow taller, beyond the shade and canopy of neighboring competitors. This selective pressure led to the conquest of land by plants through the establishment of specialized organs to support taller structures while still delivering water and nutrients. Secondary growth in plants is initiated via the vascular cambium within the stem, which supports radial growth and generates two types of vascular tissue—water-conducting xylem (wood) and assimilate-conducting phloem (bast tissue)—in opposite radial directions.

In the context of wood formation (vessels and fibers), deposition of a thick SCW composed of cellulose, lignin, and hemicellulose provides specialized functional characteristics such as mechanical strength, rigidity, and impermeability to support growth (xylem fibers) and the ability to conduct water (vessel elements) (26, 27). A hierarchical transcriptional network tightly regulates the production of the thickened SCW (28, 29). The SCW network contains master transcriptional regulators from the NAC (NAM, ATAF1/2, CUC) transcription factor family, VASCULAR-RELATED NAC DOMAIN proteins (VNDs) (30), and NAC SECONDARY WALL THICKENING PROMOTING FACTORs (NSTs) (29, 31). These SCW-associated NACs directly activate the expression of downstream transcription factor genes, including *MYB DOMAIN PROTEIN 46* (*MYB46*) and *MYB83* (32, 33), whose encoded proteins trigger the expression of SCW biosynthesis enzymes in a tissue-specific manner. Although understanding wood formation is of increasing interest given that wood accounts for the most significant proportion of terrestrial carbon sinks in land plants, and woody biomass is made up of xylem fibers (34), the specific genetic programs and signaling cues controlling NST1/3-mediated xylem fiber differentiation and whether light signaling functions in these programs remains elusive.

In this study, we identified light-directed molecular mechanisms that guide the differentiation of xylem fibers. CRY-mediated blue light signaling induces xylem fiber differentiation by repressing HY5 mobility from the shoot to the hypocotyl. CRYs interfere with HY5 translocation to hypocotyls through nuclear retention, and HY5 functions as a key long-distance suppressor of xylem fiber formation. Shoot-derived HY5 directly binds to the *NST3* promoter and prevent NST3-driven SCW deposition in xylem fibers during the initial phase of secondary growth. In addition, blue light markedly increases wood formation, such as SCW deposition and fiber elongation, in hybrid poplar. These findings provide insight into the mechanisms of light-mediated plant development via intercellular communication during secondary growth.

Results

Quantitative Anatomical Tracing of Secondary Growth in Hypocotyls Reveals That Blue Light Positively Regulates Xylem Fiber Formation. We first conducted time-lapse anatomical analysis to trace the changes in the developmental morphology of the hypocotyl during secondary growth at cellular resolution under white light (WL; Fig. 1 *A* and *B* and *SI Appendix*, Fig. S1). Analysis of cross-section images of wild-type (WT) hypocotyls showed that the areas of both hypocotyls and xylem tissue increased proportionally from 23 days after germination (DAG) to 28 DAG, with the xylem/hypocotyl area ratio remaining constant (*SI Appendix*, Fig. S1 *A*, *B*, and *D*). At 30 DAG, the rate of xylem expansion exceeded that of hypocotyl area, resulting in a higher proportion of xylem within the hypocotyl area (*SI Appendix*, Fig. S1*D*). The increase in the area of xylem II (35–37), which contains xylem fiber cells instead of parenchyma cells, resulted in a significant expansion of the ratio of xylem tissue area to hypocotyl area, which occurred at 30 DAG (after flowering) under WL (35) (Fig. 1*B* and *SI Appendix*, Fig. S1 *E*, *H*, and *I*).

To distinguish between vessels and fiber cells in xylem tissue, we analyzed images of autofluorescence signals from SCWs of each cell type (Fig. 1*C* and *SI Appendix*, Fig. S2) based on the observation that differences in lignification in these cell types (38, 39) lead to differences in the wavelengths of safranin-O autofluorescence (40). SCWs of fiber cells show autofluorescence signals mainly at 538 to 700 nm (red), with weak signals at 410 to 538 nm (green), whereas autofluorescence signals from vessel SCWs appeared at both excitation wavelengths (yellow; 410 to 700 nm) (*SI Appendix*, Fig. S2), with the same autofluorescence signal from separated vessel and fiber cells in adult hypocotyls (40). Based on our criteria, we carefully monitored vessel and fiber cell production during secondary growth. While the number of vessels increased (*SI Appendix*, Fig. S1*C*), the number of vessels per hypocotyl area did not increase, and the number of vessels per xylem tissue area significantly decreased during secondary growth (*SI Appendix*, Fig. S1*G*). By contrast, fiber cell production (xylem fiber area) and the normalized proportion of xylem fiber (xylem fiber area/hypocotyl area or xylem fiber area/xylem tissue area) significantly increased during secondary growth (*SI Appendix*, Fig. S1 *H* and *I*).

The solar elevation angle shows diurnal and seasonal fluctuations that determine the spectral composition of sunlight reaching land (*SI Appendix*, Fig. S3 *A* and *B*). We combined publicly available solar elevation angle data from a temperate climate region (Seoul) and recorded light spectrum data (41) to reconstitute the dynamics of light spectral composition (*SI Appendix*, Fig. S3 *C* and *D*). Along with the photoperiod, the proportion of different wavelengths in the light spectrum fluctuates periodically. This suggests that the light spectrum perceived by plants during the daytime may provide important light information. For instance, Ghosh et al. (42) highlighted the importance of light quality for vessel differentiation during primary growth. Thus, we quantified the effect of accumulating light spectral information on long-term secondary growth (Fig. 1 *D*–*G*). We grew *Arabidopsis* plants under equal light intensities (100 ± 3 μmol m^{-2} s^{-1}) of WL, monochromatic blue light (BL100+RL0) (peak at 453 nm), or monochromatic red light (BL0+RL100) (peak at 655 nm), all from light-emitting diode (LED) sources, under long-day conditions (Fig. 1 *D*–*G* and *SI Appendix*, Fig. S4). Notably, under BL0+RL100, xylem fibers did not develop until 30 DAG, while BL100+RL0 resulted in the expansion of xylem fibers (Fig. 1 *E* and *F*). However, vessel density (number of vessels/hypocotyl area or number of vessels/xylem area) did not correlate with the changes in vessel number under different blue/red light ratios (Fig. 1*G* and *SI Appendix*, Fig. S1 *C*, *J*, and *K*). These results indicate that the mechanism regulating xylem fiber development by blue light during secondary growth is independent of the blue light signaling pathway that controls xylem vessels during the de-etiolation process (42).

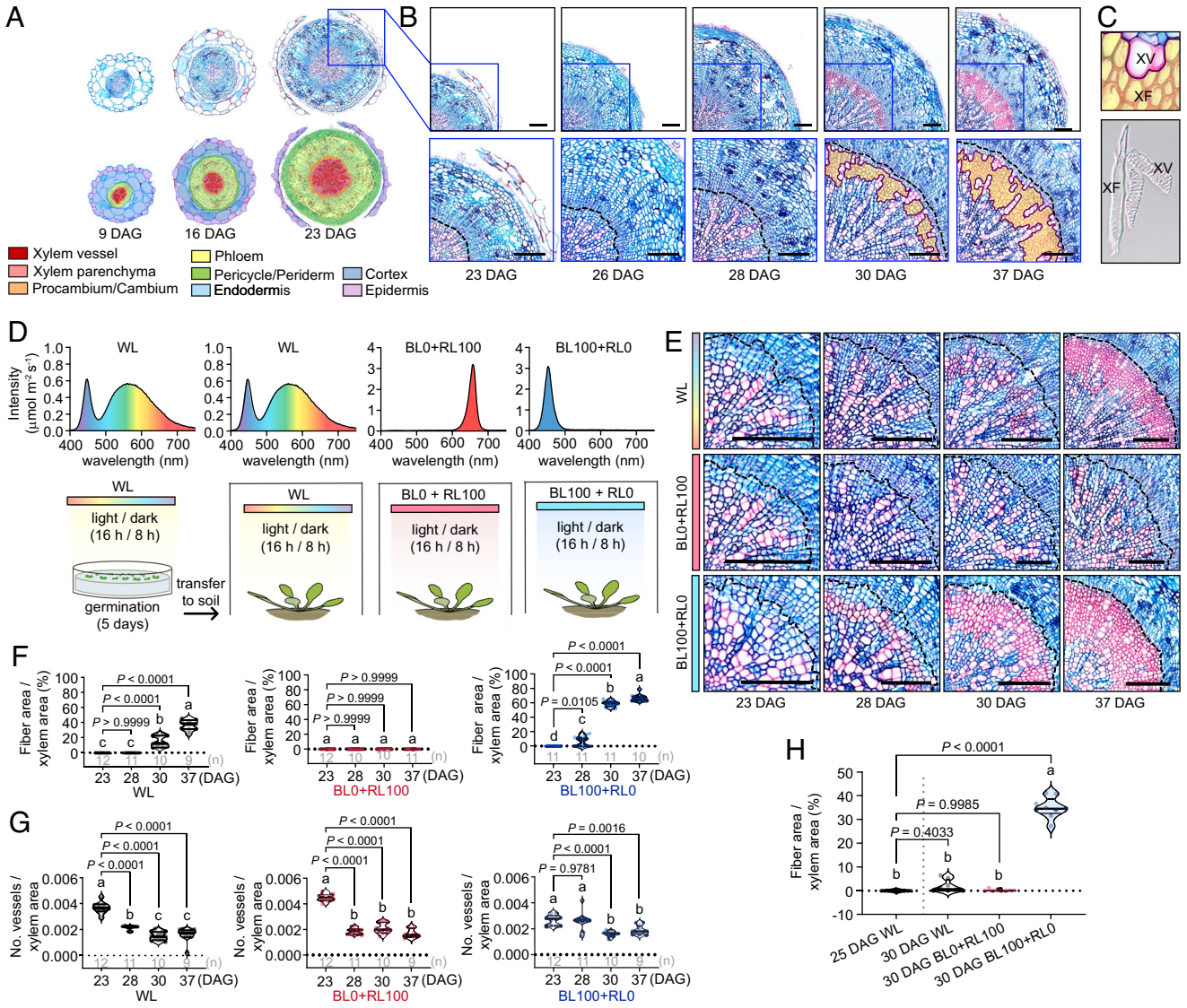

Fig. 1. Blue light accelerates xylem fiber formation independently of flowering. (*A*) cross-section images of *Arabidopsis* hypocotyls at different stages of secondary growth. Different cell types are marked with different colors. (*B*) Transverse sections of hypocotyls from WT plants grown under WL from 23 DAG to 37 DAG. Equal areas of each section are highlighted by blue boxes, and magnified views are shown in the *Lower* panel. The xylem tissue areas are indicated by dashed lines. Xylem fiber areas are outlined in purple and colored yellow. (Scale bar, 100 μm.) (*C*) Isolated xylem fiber cells and vessel elements from adult hypocotyls. XF, xylem fiber; XV, xylem vessel. (*D*) Diagrams of the light spectra for plant growth in soil used in this study. (*E*) Cross-section images of hypocotyls from WT plants at 23 DAG to 37 DAG grown under different light conditions. (Scale bar, 100 μm.) (*F* and *G*) Quantitative analysis of the cross-section images. (*F*) Percentage of xylem fiber in xylem tissue. (*G*) The number of vessels per xylem tissue area. (*H*) Quantification of the proportion of xylem fiber in xylem tissue. Data are means ± SEM ($n \geq 9$; two-way ANOVA followed by Tukey's test).

WT plants grown under each light condition showed comparable values for quantum efficiency of photosystem II, suggesting that monochromatic light (BL0+RL100 and BL100+RL0) is sufficient to maintain photosynthetic capacity until the adult stage (30 DAG), as is WL (*SI Appendix*, Fig. S5*A*). Notably, under BL40+RL60, overall growth (height, leaf shape, and leaf number) was similar to that under WL conditions (*SI Appendix*, Fig. S5*B*), suggesting minimal perturbation of plant growth due to our reconstructed light conditions with monochromatic blue and red light. Consistent with previous reports on flowering (43), blue light significantly accelerated flowering time and triggered xylem expansion in *Arabidopsis* (35) (Fig. 1 *E* and *F* and *SI Appendix*, Fig. S4). However, xylem fibers did not form at 23 DAG under BL100+RL0 or at 37 DAG under BL0+RL100 even after flowering (Fig. 1 *E* and *F* and *SI Appendix*, Fig. S4), pointing to the existence of a mechanism that regulates xylem fiber production in response to light quality in parallel or independently of flowering. Furthermore, in the late flowering mutants *constans* (*co-10*) and *flowering locus t* (*ft-10*) (44), xylem fibers still developed before flowering, but to a lesser extent than in WT under BL100+RL0 (*SI Appendix*, Fig. S6). Interestingly, short-term blue light treatment (5 d) after flowering accelerated xylem fiber production compared to the controls, suggesting that blue light participates in the early phase of xylem II expansion independently of the photoperiodic flowering pathway (Fig. 1*H* and *SI Appendix*, Fig. S5 *D* and *E*).

CRY-Dependent Blue Light Signaling Is Required for Xylem Fiber Differentiation. We then asked whether the increased xylem fiber formation in response to blue light is dependent on blue light signaling by characterizing the response of the *cry1 cry2* double mutant, which lacks functional CRY1 and CRY2—two important photoreceptors that regulate SCW deposition in inflorescence stems (45). The production of xylem fibers was completely suppressed in *cry1 cry2* under BL100+RL0, even after flowering, indicating that xylem fiber formation requires CRY-dependent blue light signaling (Fig. 2 *A* and *B* and *SI Appendix*, Figs. S5*C*

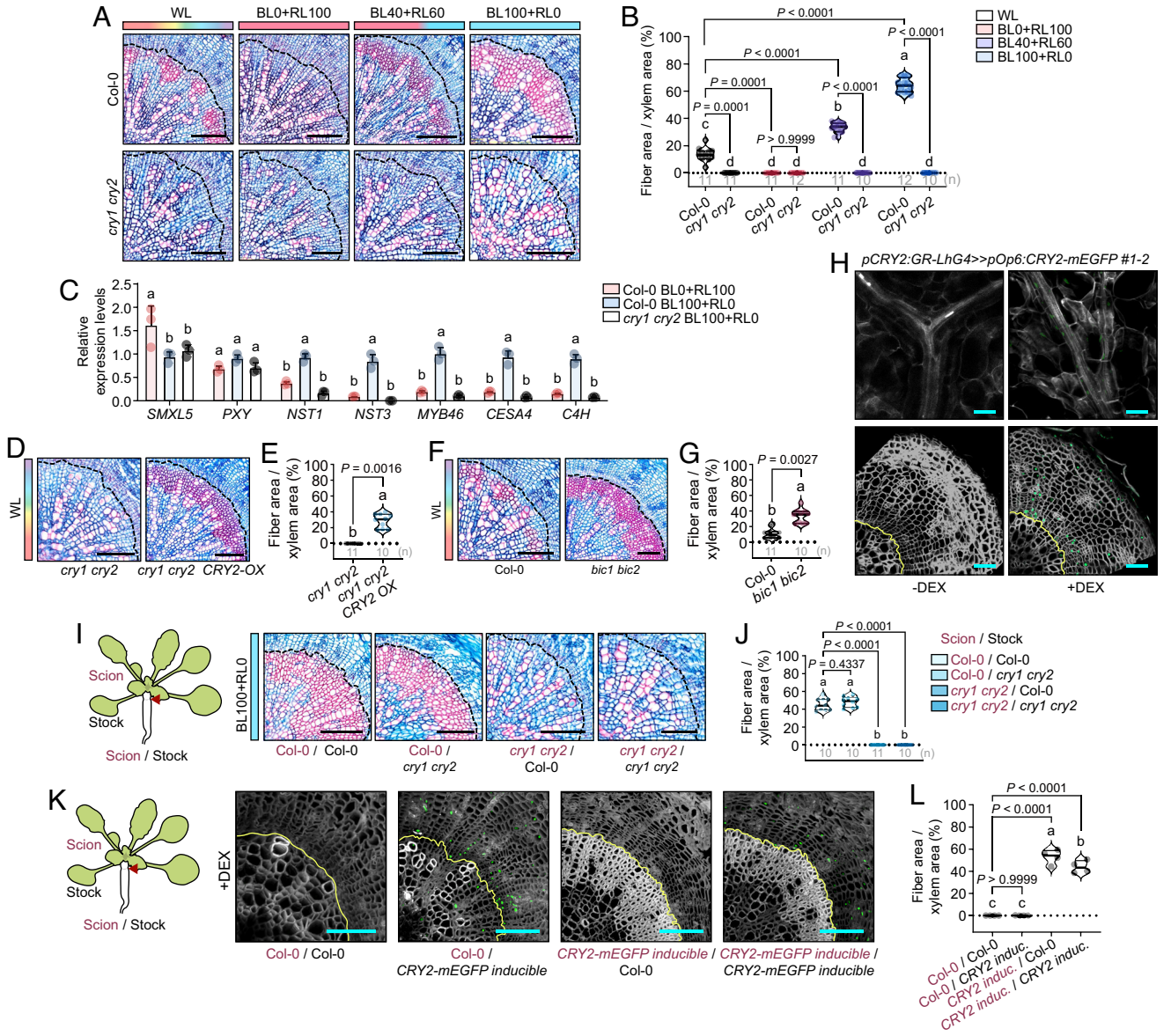

Fig. 2. The CRY-dependent blue light response is required for xylem fiber production. (*A*) Cross-section images of hypocotyl from WT and *cry1 cry2* grown under different light conditions until 30 DAG. (Scale bar, 100 μm.) (*B*) Proportion of xylem fiber to total xylem tissue. Data are means ± SEM ($n \geq 9$; two-way ANOVA followed by Tukey's test). (*C*) Relative expression levels of cambium-derived xylem tissue markers. Data are means ± SEM; different lower-case letters indicate significant differences ($n = 3$; two-way ANOVA followed by Tukey's test). (*D*) Hypocotyl cross-sections of *cry1 cry2* and *cry1 cry2 CRY2*-OX. (Scale bar, 100 μm.) (*E*) Proportion of xylem fiber in xylem tissue in *cry1 cry2* and *cry1 cry2 CRY2*-OX. Data are means ± SEM ($n \geq 10$; two-tailed Student's *t* test). (*F*) Hypocotyl cross-sections of WT and *bic1 bic2*. (Scale bar, 100 μm.) (*G*) Proportion of xylem fiber to total xylem tissue in WT and *bic1 bic2* hypocotyls. Data are means ± SEM ($n \geq 10$; two-tailed Student's *t* test). (*H*) Fluorescence signals of 23 DAG of *CRY2-mEGFP inducible* line treated with or without 20 μM DEX. Xylem areas are indicated by yellow lines. (Scale bar, 50 μm.) (*I*) Cross-sections of hypocotyl stocks from grafts between WT and *cry1 cry2* grown for 35 d after grafting. (Scale bar, 100 μm.) (*J*) Proportion of xylem fiber in hypocotyl stocks ($n \geq 10$; one-way ANOVA followed by Tukey's test). (*K*) Fluorescence signals in the hypocotyl stocks of grafted plants between WT and *CRY2-mEGFP inducible* line treated with 20 μM DEX. (Scale bar, 100 μm.) (*L*) Proportion of xylem fiber in xylem of grafted chimeras ($n \geq 10$; one-way ANOVA followed by Tukey's test).

and S7). The *cry1* and *cry2-1* single mutants formed normal xylem fibers in BL100+RL0, pointing to functional redundancy between the two photoreceptors (*SI Appendix*, Fig. S8 *A* and *B*). Furthermore, as we observed no xylem fibers in plants grown under BL0+RL100, we asked whether this lack of development represents active phy-mediated repression by examining xylem fiber differentiation in *phy* mutants (*SI Appendix*, Fig. S8 *C* and *D*). The loss-of-function mutants *phyA-211* and *phyB-9* did not show any differences in xylem fiber formation compared to the control in any light condition, supporting the notion that xylem fiber differentiation requires a CRY-dependent blue light signal. In agreement with the results of histological analysis, the expression of the master regulators of xylem fiber formation and SCW-related genes was significantly induced by blue light in a CRY-dependent manner, suggesting that blue light signaling is crucial for regulating vascular tissue differentiation (Fig. 2*C*). Moreover, analysis of fiber formation in plants overexpressing *CRY2* in the *cry1 cry2* background, as well as plants lacking functional BLUE LIGHT INHIBITOR OF CRYPTOCHROMEs (BICs) (46), indicated that CRY-dependent blue light signaling is essential for xylem fiber formation during hypocotyl secondary growth (Fig. 2 *D*–*G*).

Next, we asked whether light functions locally or as a long-distance signal for fiber differentiation. To examine this issue,

we performed reciprocal grafting between 5-d-old WT and *cry1 cry2* in which we grafted shoot apical meristems (scions) from one genotype onto hypocotyl stocks from the other genotype. 35 d later, we collected hypocotyls from the stocks and produced cross-sections below the hypocotyl grafting junction for analysis (Fig. 2 *I* and *J* and *SI Appendix*, Fig. S9). Hypocotyl stocks of WT showed defective xylem fibers when grafted to *cry1 cry2* scions, whereas grafting a WT scion onto a *cry1 cry2* stock fully rescued the xylem fiber formation and shoot phenotypes (Fig. 2 *I* and *J* and *SI Appendix*, Fig. S9). This result indicates that CRYs determine the xylem fiber formation of the hypocotyl in the shoot. To visualize CRY2 protein accumulation during primary and secondary growth, we generated an inducible translational reporter line of CRY2 (*CRY2-mEGFP inducible*) using the glucocorticoid receptor (GR)-fused LhG4/pOp transactivation system (47) (Fig. 2*H* and *SI Appendix*, Fig. S14 *A* and *C*). The chimeric transcription factor LhG4 under the control of the *CRY2* promoter induced *CRY2-mEGFP* reporter expression driven by the multiple interspersed repeats of the lac operator elements (*pOp6*) after dexamethasone (DEX) treatment to induce reporter expression. CRY2-mEGFP accumulation was observed in both mesophyll cells and vascular tissues in adult shoots after DEX treatment (Fig. 2*H*). In addition, DEX treatment rescued the late flowering phenotype and defective xylem fibers of *cry1 cry2* (*SI Appendix*, Fig. S14 *D* and *E*). CRY2-mEGFP was also observed in cambium-related cell types in the hypocotyl (distal and proximal cambium areas) (48) (Fig. 2*H*). Given this expression profile, we reasoned that the CRY2 in the hypocotyl might function autonomously in xylem fiber formation, irrespective of long-distance signaling. To distinguish between long-distance signaling and local signaling mediated by CRYs, we performed grafting experiments using the *CRY2-mEGFP inducible* line (Fig. 2 *K* and *L*). Remarkably, after DEX treatment, WT stock displayed significant increased xylem fiber production, while CRY2-mEGFP fluorescence signal was not detected when WT stock was grafted to *CRY2-mEGFP inducible* scions. By contrast, chimeric plants comprising *CRY2-mEGFP inducible* stock and WT scion showed a similar xylem fiber formation phenotype to WT self-chimeras (Fig. 2 *K* and *L*). These results further support the notion that a shoot-derived, long-distance CRY-mediated blue light signal determines xylem fiber differentiation in the adult hypocotyl.

CRY-Mediated Blue Light Signaling Activates SCW-Related Gene Expression while Suppressing Cell Cycle–Related Gene Expression in Adult Hypocotyls. Since the blue light signal travels from the shoot to the hypocotyl to induce xylem fiber formation, we performed bulk RNA-seq analysis using adult hypocotyls from WT and *cry1 cry2* (*SI Appendix*, Figs. S10 and S11*A*) grown under different light conditions (BL0+RL100 and BL100+RL0) (49). Principal component analysis and Pearson's correlation analysis of all samples validated the high quality of our data (*SI Appendix*, Fig. S10 *A* and *B*). We identified 4,183 CRY-dependent differentially expressed genes (DEGs) based on a comparison between BL100+RL0 Col-0 and BL100+RL0 *cry1 cry2* samples (*SI Appendix*, Fig. S10*C*); we also detected 2,386 blue light–dependent DEGs between Col-0 BL100+RL0 and Col-0 BL0+RL100. Of these, 1,746 genes were identified as blue light– and CRY-dependent DEGs in the adult hypocotyl (*SI Appendix*, Fig. S11*A*). Remarkably, 96.5% of these genes were coregulated by CRYs and the blue light signal, including 1,162 co-up-regulated DEGs and 523 co-down-regulated DEGs (*SI Appendix*, Figs. S10*C* and S11*B* and Dataset S1). These results suggest that the changes in gene expression mediated by blue light in the adult hypocotyl are almost entirely dependent on CRY activity.

Hierarchical clustering and gene ontology (GO) analysis of the blue light CRY–dependent DEGs showed that the co-up-regulated genes (cluster 1) were enriched in the GO terms "secondary metabolic process," "phenylpropanoid metabolic process," "secondary cell wall biogenesis," and "xylan or lignin biosynthetic process" (*SI Appendix*, Fig. S11 *C* and *D*), strongly suggesting that SCW deposition is a major event in CRY-dependent blue light-induced xylem fiber formation. DEGs co-down-regulated by blue light and CRYs (cluster 2+3) were associated with "cell division," "cell cycle," "regulation of transferase activity," and "hydrogen peroxide catabolic process" (*SI Appendix*, Fig. S11 *C* and *E*), supporting the notion that blue light– and CRY-dependent signaling inhibits cambial cell division (*SI Appendix*, Fig. S11*E*). Consistent with this notion, we observed a significant difference in the expression patterns of DEGs involved in SCW biosynthesis and cell division upon blue light exposure (*SI Appendix*, Fig. S11 *F* and *G*). These results confirm that blue light and CRYs positively regulate xylem fiber development while suppressing cell division activity.

Next, to explore whether the expression profiles of blue light-CRY–responsive genes in the adult hypocotyl identified in our analysis changed over time, we compared our results with transcriptomic data from a previous study of *cry1 cry2* seedlings grown under blue-light conditions (50) (*SI Appendix*, Fig. S11*H*). Among the 1,728 DEGs identified in the comparison between WT and *cry1 cry2* seedlings, a subset of 554 DEGs overlapped with DEGs identified in adult hypocotyls, accounting for approximately 13% of the 4,183 DEGs identified in adult hypocotyls (*SI Appendix*, Fig. S11 *H* and *K*). This result indicates that the blue light-CRYs module governs distinct mechanisms at different stages of development. To elucidate the biological significance of the unique DEGs in the adult hypocotyl, we performed GO analysis on the remaining 3,629 DEGs that were differentially expressed exclusively in this tissue. Of the 3,629 DEGs examined, 50% (1,830) were up-regulated by blue-light CRY signals and were associated with lignin metabolic process and secondary cell wall biogenesis (*SI Appendix*, Fig. S11*I*). The 554 DEGs that were commonly regulated in both seedlings and adult hypocotyls were categorized into four subgroups (*SI Appendix*, Figs. S10 *D*–*F* and S11*L*). One of these subgroups (group 3; 106 genes) was associated with "Plant-type secondary cell wall" (*SI Appendix*, Fig. S11*L*). The expression of these DEGs was reduced in seedlings in a blue light-CRYs-dependent manner, in contrast to adult hypocotyls (*SI Appendix*, Fig. S11 *K* and *L*). This reduction aligns with previously generated time-lapse light-dependent gene expression profiles at the single-cell level (51). These results indicate that the blue light-CRYs module acts as a dual regulator in the hypocotyl, functioning as a suppressor in seedlings and as an activator in adult hypocotyls depending on the developmental stages in the context of SCW formation. On the contrary, the "cell division" and "cell cycle" regulatory pathways were down-regulated by the blue light-CRYs module regardless of developmental stage (*SI Appendix*, Figs. S10*D* and S11*J*).

In light of the effect of CRY-mediated blue light signaling on the expression of SCW biosynthetic genes during xylem fiber development, we analyzed the promoters of the blue light-CRY–dependent DEGs (Dataset S2) for specific *cis*-elements that might reveal their upstream transcription factors (52). The ACGT-element (ACE motif) was enriched in DEGs commonly up-regulated by blue light/CRYs in adult hypocotyls; this element is highly similar to the binding site of the bZIP transcription factor HY5 (*SI Appendix*, Fig. S11*M*). Based on these findings, we propose that HY5 acts as a key transcription factor that mediates the role of CRY-dependent blue light signaling in xylem fiber production.

HY5 Negatively Regulates the Expression of CRY-Dependent Blue Light–Responsive SCW Genes Involved in Xylem Fiber Formation. To assess the effect of HY5 on xylem fiber differentiation, we examined the extent of fiber formation in the *hy5* mutant and *HY5* overexpression lines in the *hy5* background (*hy5 HY5-GFP*-OX) under different light conditions (Fig. 3 *A* and *B*). The *hy5* mutant showed significantly more xylem fiber development and *hy5 HY5*-GFP-OX plants exhibited less xylem fiber development than WT plants, indicating that HY5 negatively regulates xylem fiber formation in adult hypocotyls (Fig. 3 *A* and *B* and *SI Appendix*, Fig. S12*A*). The *hy5-ks50* mutant in the Ws-2 background also showed increased xylem fiber formation. HY5 does not play redundant roles with the related transcription factor, HY5 HOMOLOG (HYH) (53), as the *hyh* mutant exhibited a similar degree of fiber formation to the WT (*SI Appendix*, Fig. S12 *B* and *C*), and the *hy5-ks50 hyh* double mutant resembled *hy5* in terms

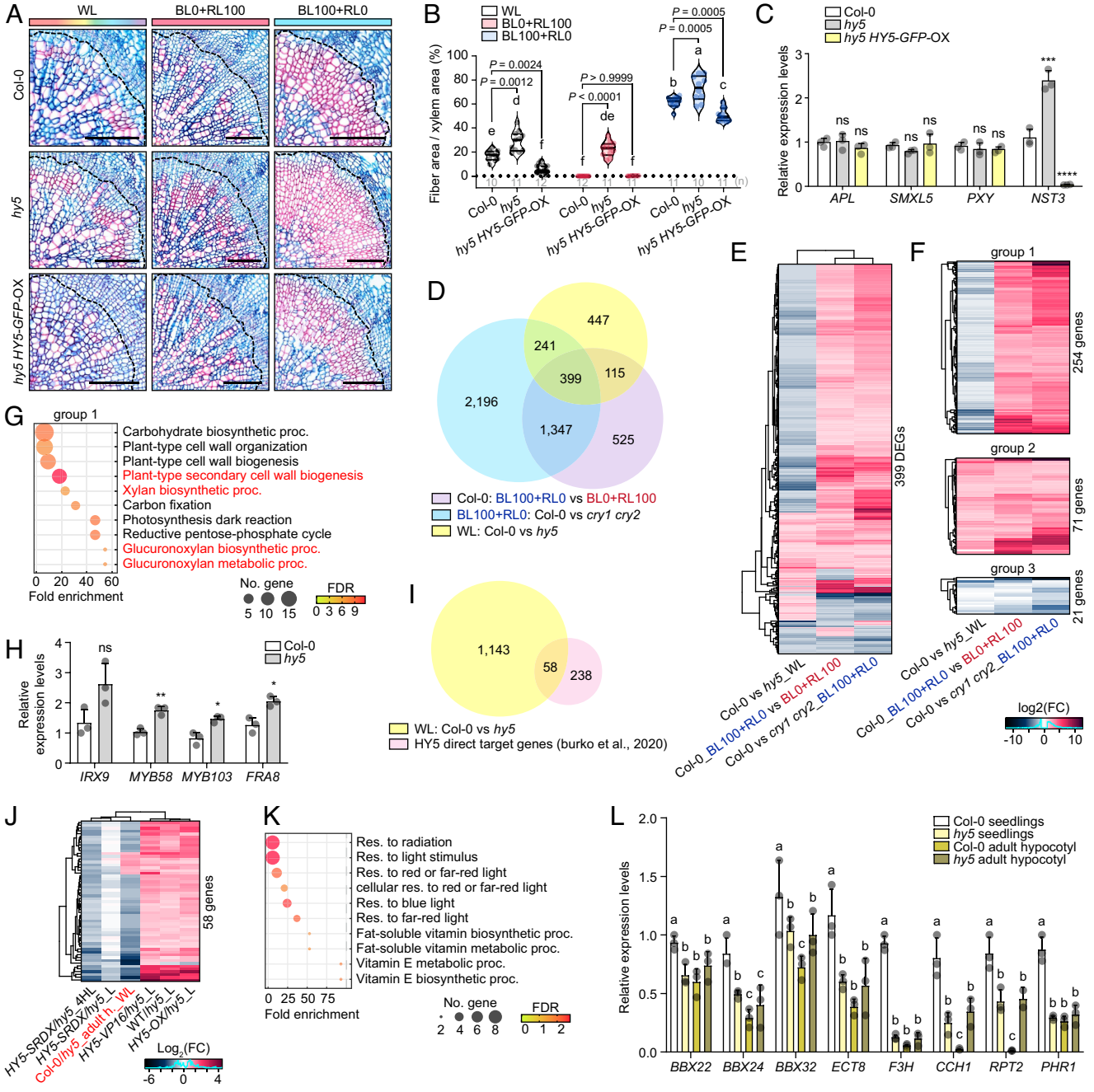

Fig. 3. HY5 negatively regulates the effect of CRY-dependent blue light signaling on xylem fiber formation via its transcriptional repressor activity. (*A*) Hypocotyl cross-sections of Col-0, *hy5*, and *hy5 HY5-GFP*-OX. (Scale bar, 100 μm.) (*B*) Proportion of xylem fiber to xylem in Col-0, *hy5*, and *hy5 HY5-GFP*-OX. Data are means ± SEM ($n \geq 10$, two-way ANOVA followed by Tukey's test). (*C*) Relative expression levels of cambium-derived vascular tissue marker genes. Data are means ± SEM ($n = 5$; ****$P < 0.0001$; ns, not significant, two-tailed multiple Student's *t* test). (*D*) Venn diagram showing the number of DEGs in response to light quality, *cry1 cry2* under BL100+RL0, and *hy5* under WL. (*E*) Heat map of blue light-CRY-HY5 responsive DEGs (399 genes). (*F*) Heat map of 346 DEGs (groups 1 to 3) that are differentially expressed in response to blue light-CRY or HY5. (*G*) Enriched GO terms of group 1 DEGs. SCW-associated categories are shown in red. (*H*) Relative expression levels of SCW biosynthesis-associated DEGs down-regulated by HY5. Data are means ± SEM ($n = 5$; ****$P < 0.0001$; ns, not significant, two-tailed multiple Student's *t* test). (*I*) Venn diagram showing the number of direct target genes of HY5 in seedlings and HY5-responsive genes in adult hypocotyls. (*J*) Heat map showing the differential expression of direct targets of HY5 (58 genes). HY5-responsive genes in adult hypocotyls are shown in red. (*K*) Enriched GO terms of direct target genes of HY5 down-regulated by HY5 in adult hypocotyls. (*L*) Relative expression levels of direct target genes of HY5 in seedlings and adult plants. Data are means ± SEM; different lower-case letters indicate significant differences ($n = 5$; two-way ANOVA followed by Tukey's test).

of xylem fiber development (*SI Appendix*, Fig. S12 *B* and *C*). In agreement with their observed phenotypes, *NST3* was significantly up-regulated in *hy5* and *hy5-ks50*, while *HY5* overexpression strongly diminished *NST3* expression in the hypocotyl compared to the controls (Fig. 3*C* and *SI Appendix*, Fig. S12*D*). These results confirm that HY5 plays a major role in the suppression of xylem fiber formation (Fig. 3 *A*–*C* and *SI Appendix*, Fig. S12).

Given that HY5 is a central repressor of xylem fiber formation irrespective of the light spectrum, we investigated whether HY5 contributes to the expression of xylem fiber–related genes that are up-regulated in response to CRY-dependent blue light signaling. We performed bulk RNA-seq to identify HY5-responsive genes in the adult hypocotyl (30 DAG) (*SI Appendix*, Fig. S12 *E* and *F* and Dataset S1) and compared them to the CRY-dependent blue light–responsive DEGs (Fig. 3*D*). Among the 1,202 DEGs in *hy5*, the up-regulated genes in *hy5* were highly enriched in the GO term "plant-type secondary cell wall" (*SI Appendix*, Fig. S12*G*). We also identified 399 blue light–, CRY-, and HY5-dependent genes (Fig. 3 *D* and *E*). We verified the enriched GO terms for 86.7% of the 399 DEGs, which were divided into three groups based on their expression patterns (13.3% of DEGs were not significantly enriched for any GO terms) (Fig. 3 *E* and *F*). Among these, 254 DEGs (group 1) were up-regulated by CRY-dependent blue light but down-regulated by HY5. These genes were enriched in the GO terms "Plant-type secondary cell wall" and "xylan biosynthesis," supporting a role of HY5 as an inhibitor of light-induced xylem fiber formation in the adult hypocotyl (Fig. 3*G*). In line with this finding, we confirmed significant differences in expression of DEGs associated with SCW biosynthesis in an HY5-dependent manner (Fig. 3*H*). The DEGs that exhibited identical expression patterns that were dependent on blue light-CRYs and HY5 (group 2 and group 3) were mainly associated with defense, stress response, and regulation of stomatal movement (*SI Appendix*, Fig. S12 *I* and *J*).

HY5 acts as a positive regulator of direct target genes to regulate photomorphogenesis during primary growth (54). This finding prompted us to investigate whether HY5 functions as a repressor of light-responsive genes in the adult hypocotyl, which is not observed in seedlings. Of the 297 light-responsive direct target genes of HY5 (54), 58 genes showed HY5-dependent differences in expression in the adult hypocotyl, and are all positively regulated by HY5 during primary growth (Fig. 3*I*). Intriguingly, approximately 84.5% (49 DEGs) of these DEGs were down-regulated by HY5 during secondary growth and are light-responsive genes (Fig. 3 *J* and *K*). We validated the expression patterns of direct target genes of HY5 at specific developmental stages in WT and *hy5* plants (Fig. 3*L*). Consistent with previous findings, the expression of these genes was reduced in *hy5* seedlings compared to WT seedlings. Interestingly, *BBX32*, *CCH1*, and *RPT2* showed significantly increased expression in the adult hypocotyls of *hy5* compared to WT (Fig. 3*L*). These results suggest that HY5 has dual roles at different developmental stages, acting as a negative regulator of secondary growth in adult hypocotyls.

To explore the regulation of developmental stage–specific gene expression by HY5, we compared the 1,179 DEGs from seedlings (54) with 1,202 DEGs from adult hypocotyls (*SI Appendix*, Fig. S13). All but 178 DEGs exhibited differential expression exclusively during either primary or secondary growth, with genes associated with the "Plant-type secondary cell wall" regulated by HY5 specifically during secondary growth (*SI Appendix*, Fig. S13). These findings indicate that HY5 acts as a negative regulator of secondary growth and that its role in negatively regulating xylem fiber formation is restricted to the adult stage. In addition, the increased xylem fiber development in *hy5* was no longer observed in later stages of secondary growth, suggesting that HY5 regulates xylem fiber formation at the initial phase of secondary growth (*SI Appendix*, Fig. S12*A*). Collectively, these results suggest that HY5 acts as a repressor of CRY-dependent blue light–mediated xylem fiber production, which prompted us to explore a suite of mechanisms controlled by CRYs.

CRY Proteins Are Associated with Nuclear Retention of HY5, Potentially Affecting Its Long-Distance Shoot-to-Hypocotyl Translocation during Secondary Growth. To trace the HY5 protein accumulation profile, we generated an inducible translational reporter line of HY5 (*HY5-mEGFP inducible*) using the GR-fused LhG4/pOp transactivation system (47). As previously reported (55), HY5 was detected throughout the plant during primary growth. HY5 accumulated in the mesophyll and leaf veins of cotyledons in seedlings, as well as the shoot apical meristem, except for the L1 layer. From the hypocotyl to the root, HY5 accumulation was predominantly observed in the vasculature (*SI Appendix*, Fig. S14 *B* and *C*). We then monitored HY5 accumulation in adult plants. DEX treatment in soil induced HY5-mEGFP accumulation in leaf veins of adult shoots and suppressed xylem fiber formation (Fig. 4*A* and *SI Appendix*, Fig. S14*F*). HY5 protein was also observed in the xylem parenchyma and phloem area in the adult hypocotyl (Fig. 4*A*). Compared to the light quantity reaching the shoot, the hypocotyl experienced extremely low light conditions, indicating that local HY5 in the adult hypocotyl is less capable of transducing light information than HY5 in the shoot. This suggests that HY5 in the hypocotyl might function as a long-distance signaling protein, conveying light information to belowground tissues such as the root (*SI Appendix*, Fig. S15 *A*–*C*). To determine whether non-cell-autonomous or local HY5 is involved in xylem fiber formation, we performed grafting experiments using independent HY5 transgenic lines (Fig. 4 *B* and *C* and *SI Appendix*, Figs. S15 *D*–*F* and S18 *A* and *B*). After DEX treatment, WT stock displayed significantly reduced xylem fiber formation when grafted to *HY5-mEGFP inducible* scions, whereas chimeras of *HY5-mEGFP inducible* stock and WT scion did not show differences in xylem fiber formation compared with WT self-chimeras (Fig. 4*B* and *SI Appendix*, Fig. S15*D*). In addition, *HY5-GFP-OX* scions suppressed xylem fiber development in hypocotyl stocks of *hy5* compared to *hy5* self-grafts, further supporting the notion that shoot-derived HY5 inhibits fiber formation in a non-cell-autonomous manner (*SI Appendix*, Fig. S15 *E* and *F*).

To further examine the mobility of HY5, we monitored HY5 protein accumulation in adult hypocotyls using chimeric plants comprising WT stocks and *HY5-mEGFP inducible* scions. The HY5-mEGFP signal in WT stock occurred at a higher frequency than that from *HY5-mEGFP inducible* stock and at a similar frequency to that observed in self-grafted *HY5-mEGFP inducible* stock (Fig. 4*B*). Similarly, HY5-HA and HY5-GFP, originating from *pHY5:HY5-HA* and *HY5-GFP-OX* scions, respectively, accumulated in the hypocotyl stocks of both WT and *hy5* (Fig. 4*C* and *SI Appendix*, Fig. S18 *A* and *B*). These results strongly support the notion that the long-distance translocation of HY5 from the shoot to the hypocotyl contributes to the inhibition of xylem fiber differentiation. In the vasculature of the adult petiole, we detected cytosolic HY5 protein within the procambium region, supporting the notion that HY5 can be transported over long distances from the shoot to the hypocotyl via the vasculature (Fig. 4*D*).

To investigate the impact of CRYs on the subcellular localization of HY5, we conducted a fractionation experiment with adult shoot petioles of *pHY5:HY5-HA* lines in both the WT and *cry1 cry2* backgrounds. Subsequently, we performed immunoblot

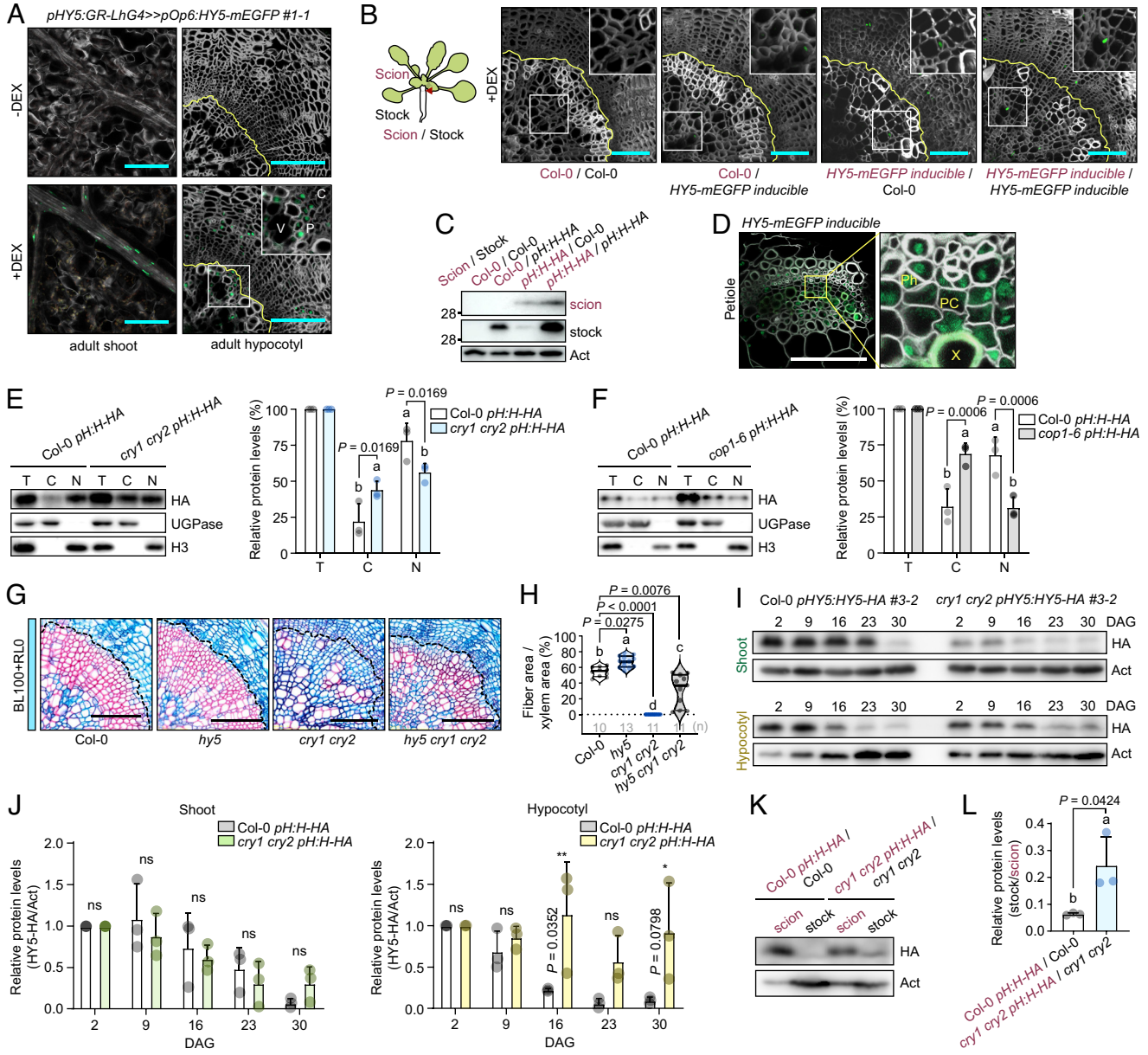

Fig. 4. CRYs inhibit the long-distance mobility of HY5 by retaining it in the nucleus. (*A*) Fluorescence signals of adult *HY5-mEGFP inducible* line. (*B*) Fluorescence signals from hypocotyl stocks of the grafted chimeras between WT and *HY5-mEGFP inducible* line. (*C*) Representative images of immunoblots; protein extracts from the indicated tissues of grafted plants were separated by 12.5% SDS-PAGE. (*D*) Fluorescence signals in cross-sections of petioles from the *HY5-mEGFP inducible* line. Ph, phloem; PC, procambium; X, xylem. (*E* and *F*) *Left* panel; Representative images of immunoblots of the nucleus-cytosol fractions from adult shoot petioles of Indicated plants. *Right* panel; quantification of relative HY5-HA levels (n = 3; one-way ANOVA followed by Tukey's test). (*G*) Hypocotyl cross-sections of Col-0, *hy5*, *cry1 cry2*, and *hy5 cry1 cry2*. (*H*) Proportion of xylem fiber area to xylem area in Col-0, *hy5*, *cry1 cry2*, and *hy5 cry1 cry2* ($n \geq 10$; one-way ANOVA followed by Tukey's test). (*I*) Representative images of immunoblots from indicated plants at different developmental stages. (*J*) Relative protein abundance of HY5-HA in the shoot or hypocotyl, normalized to Actin levels. (*K*) Representative images of immunoblots of protein extracts from the indicated tissues of grafted plants. (*L*) Relative abundances of proteins in the stock versus the scion. Data are means ± SEM ($n = 3$; $^*P < 0.05$; two-tailed multiple Student's *t* test). HY5-HA protein was visualized with anti-HA antibody. Enrichment of the nuclear and cytosol fractions was determined by probing with anti-H3 antibody and anti-UGPase antibody, respectively. *pH:H-HA* refers to *pHY5-HY5-HA*. T, Total; C, Cytosol-enriched fraction; N, Nucleus-enriched fraction. (Scale bar, 100 μm.)

analysis of the nuclear and cytosolic fractions (Fig. 4*E*). Although the total HY5 protein level was lower in *cry1 cry2* than in WT seedlings (*SI Appendix*, Fig. S16 *B* and *C*) but was similar in adult petioles. Interestingly, the cytosolic/nuclear HY5 abundance ratio was higher in *cry1 cry2* than in the WT, demonstrating that CRYs help mediate the nuclear localization of HY5 (Fig. 4*E* and *SI Appendix*, Fig. S18*D*). In addition, the total HY5 protein level increased in the *cop1-6* background, but the proportion of cytosolic HY5 versus nuclear HY5 also significantly increased in the *cop1-6* background compared to WT (Fig. 4*F* and *SI Appendix*, Fig. S18*E*). CRY2-induced nuclear retention of HY5 was also significantly attenuated in the *cop1-6* background compared to WT (*SI Appendix*, Figs. S17 *C* and *D* and S18 *F* and *G*). By contrast, *COP1* overexpression increased the nuclear localization of HY5 in the light (*SI Appendix*, Figs. S17*E* and S18*H*). Therefore, we propose that CRY-mediated nuclear retention of HY5 requires COP1, potentially through CRYs–COP1–HY5 complex formation in the nucleus. To genetically dissect the role of HY5 in CRY-dependent fiber formation, we generated the *hy5 cry1 cry2* triple mutant by genetic crossing and examined its xylem fiber development under BL100+RL0 (Fig. 4 *G* and *H* and *SI Appendix*, Fig. S16 *D*–*H*). The defect in xylem fiber formation was partially rescued in *hy5 cry1 cry2* compared to *cry1 cry2*, indicating that HY5 suppresses xylem fiber formation downstream of (or in

parallel to) CRY-dependent blue light signaling (Fig. 4 *G* and *H*). Furthermore, reciprocal grafting using *hy5* and *cry1 cry2* confirmed that the genotype of the shoot is a key determinant of xylem fiber formation in hypocotyls (*SI Appendix*, Fig. S17 *A* and *B*). This also suggests that shoot-derived HY5 likely moves to the hypocotyl more efficiently in *cry1 cry2* than the WT. Finally, the *cop1-6* mutant exhibited a defect in xylem fibers similar to that of the *cry1 cry2* mutant (*SI Appendix*, Fig. S17*F*), supporting the idea that COP1 is involved in CRY-mediated xylem fiber production, at least in part through HY5 translocation.

Based on the results of genetic, biochemical, and grafting experiments, we reasoned that spatiotemporal CRY-dependent blue light signaling in the shoot controls the mobility of HY5 from shoot to hypocotyl, strongly affecting xylem fiber formation. To examine this hypothesis, we monitored changes in HY5 protein levels in shoots and hypocotyls over time (Fig. 4 *I* and *J*). In the WT background, HY5 protein accumulation gradually decreased over time in both shoots and hypocotyls (Fig. 4 *I* and *J* and *SI Appendix*, Fig. S18*C*). Unexpectedly, HY5 protein accumulation in hypocotyls significantly increased in the *cry1 cry2* background compared to WT hypocotyls after 16 DAG (Fig. 4 *I* and *J* and *SI Appendix*, Fig. S18*C*). There are two possible explanations for this discrepancy. First, CRYs could play a role in preventing the movement of HY5 from shoot to hypocotyl; second, local CRYs might suppress HY5 protein accumulation specifically in the hypocotyl. To examine the possible roles of CRYs in HY5-mediated xylem fiber formation, we conducted experiments using scions carrying the *pHY5:HY5-HA* transgene in the WT and *cry1 cry2* backgrounds grafted onto WT and *cry1 cry2* stocks, respectively (Fig. 4 *K* and *L* and *SI Appendix*, Fig. S18*I*). Analysis of shoot-derived HY5 protein accumulation in the hypocotyl stocks versus the scion revealed significant increases in hypocotyls of *cry1 cry2* compared to WT stocks (Fig. 4 *K* and *L* and *SI Appendix*, Fig. S18*I*). These results collectively suggest that CRYs inhibit the long-distance translocation of HY5 in the hypocotyl during secondary growth.

Shoot-Derived HY5 Inhibits Xylem Fiber Formation by Directly Binding to the Promoter of *NST3*, Encoding a Master Transcriptional Regulator of SCW Formation. The transcription factors NST1 and NST3 (also named SECONDARY WALL-ASSOCIATED NAC DOMAIN 1 [SND1]) are key players in the selective activation of SCW formation for xylem development (29, 31). *NST3* expression was induced by CRY-mediated blue light signaling but repressed by HY5 in the hypocotyl (Figs. 2*C* and 3*C* and *SI Appendix*, Fig. S12*D*), while *NST1* expression was unaltered in the *hy5* background (Dataset S1). We thus hypothesized that HY5-NST3 bridges light signaling and xylem fiber formation. To determine whether HY5 directly binds to the *NST3* promoter, we looked for HY5 binding motifs (G-box and variants) in the *NST3* promoter and identified three bZIP-type binding motifs (ACGTCA) within the 1-kb promoter region upstream of ATG (Fig. 5*A*). We performed an electrophoretic mobility shift assay (EMSA) with two *NST3* promoter fragments containing bZIP-binding motifs (Probe 1 and 2) (Fig. 5 *A* and *B*). Recombinant glutathione *S*-transferase (GST)-HY5 retarded the mobility of *NST3* probes 1 and 2, but not the mutated probes (mProbes 1 and 2); unlabeled competitors completely abolished these mobility shifts. These results indicate that HY5 directly binds to the *NST3* promoter through the bZIP-binding motif (Fig. 5*B*). To confirm the direct binding of HY5 to the *NST3* promoter in vivo, we conducted a dual-luciferase (LUC) reporter assay using a reporter construct harboring the firefly luciferase (Fluc) reporter gene driven by the *NST3* promoter. Coexpression of *HY5-VP16*, encoding a chimeric transcriptional activator form of HY5, significantly induced LUC activity from the *pNST3:Fluc* reporter. However, coexpression of *HY5-VP16* with a mutated version of the *NST3* promoter lacking bZIP-binding sites (*pNST3m1/2/3*, full mutated version) failed to increase the LUC activity of the reporter (Fig. 5*C*). Collectively, these data indicate that HY5 directly recognizes the *NST3* promoter.

To further examine the role of HY5 in negatively regulating *NST3* expression (Fig. 3*C* and *SI Appendix*, Fig. S12*D*), we performed a LUC reporter assay using *pNST3:Fluc* reporter fused to a minimal *35S* promoter (Fig. 5*D*). The activity of the reporter was strongly compromised by the HY5-HA protein, indicating that HY5 directly binds to *NST3* and suppresses its expression (Fig. 5*D*). In addition, we performed a CUT&RUN assay using *pHY5:HY5-HA* seedlings and found that HY5 directly binds to the ACE motifs in the *NST3* promoter in vivo (Fig. 5*E*). We then performed genetic analysis of the role of HY5 in *NST3*-mediated xylem fiber formation by introducing the *hy5* mutation into the *nst1-1 nst3-1* double mutant background (Fig. 5 *F* and *G* and *SI Appendix*, Fig. S19). The *hy5* mutant showed increased xylem fiber formation, which was completely abolished in the *hy5 nst1 nst3* triple mutant, indicating that HY5 functions upstream of *NST3*-driven xylem fiber formation (Fig. 5 *F* and *G*). Remarkably, transgenic plants expressing *NST3* driven by the mutated version of the *NST3* promoter (and thus independent of HY5) in the *nst1-1 nst3-1* double mutant background showed xylem fiber production in hypocotyls even in the absence of blue light, supporting the notion that the direct HY5-mediated suppression of *NST3* expression is critical for repressing xylem fiber differentiation (Fig. 5 *H* and *I*).

Blue Light Increases SCW Deposition and Cell Elongation in Poplar Xylem Fiber. We closely monitored the effect of light on the development of xylem fibers in hybrid poplar, given that xylem fibers are a major component of wood (56). We grew poplar (*Populus alba* × *Populus glandulosa*) under different light conditions (*SI Appendix*, Figs. S20 and S21). We transferred trees grown under WL to BL100+RL0 or BL0+RL100 and grew them for 3 wk (*SI Appendix*, Figs. S21*A*). To track developmental differences over the 3-wk period, we designated the apical region of poplar as the starting point before altering light conditions, unlike typical methods (*SI Appendix*, Fig. S20*A*). Compared to poplars grown under red light, blue light induced stem elongation and increased the number of developed nodes (*SI Appendix*, Fig. S20 *B* and *C*). To accurately interpret the effects of blue light on stem elongation, we examined the development of all nodes and internodes in detail. Blue light induced the elongation of all internodes, leading to significant increases in node length compared to plants grown under red light (*SI Appendix*, Fig. S20 *D* and *E*). However, differences in light quality did not result in significant differences in stem area (*SI Appendix*, Fig. S20*F*).

We then observed the impact of blue light on the development of the xylem axial system (34). Consistent with our findings in *Arabidopsis*, blue light accelerated xylem differentiation in poplar (*SI Appendix*, Fig. S21*B*). In internode 10, blue light triggered the expansion of xylem precursor cells within the interfascicular vasculature. Additionally, the initiation of SCW accumulation in libriform fiber cells occurred in both the fascicular and interfascicular regions of internode 9 (*SI Appendix*, Fig. S21*B*), suggesting that blue light accelerates libriform fiber differentiation in poplar. To investigate the impact of blue light on the expression of genes related to xylem development and SCW formation, we analyzed the expression levels of essential enzyme-encoding genes and the upstream transcription factors that regulate their expression

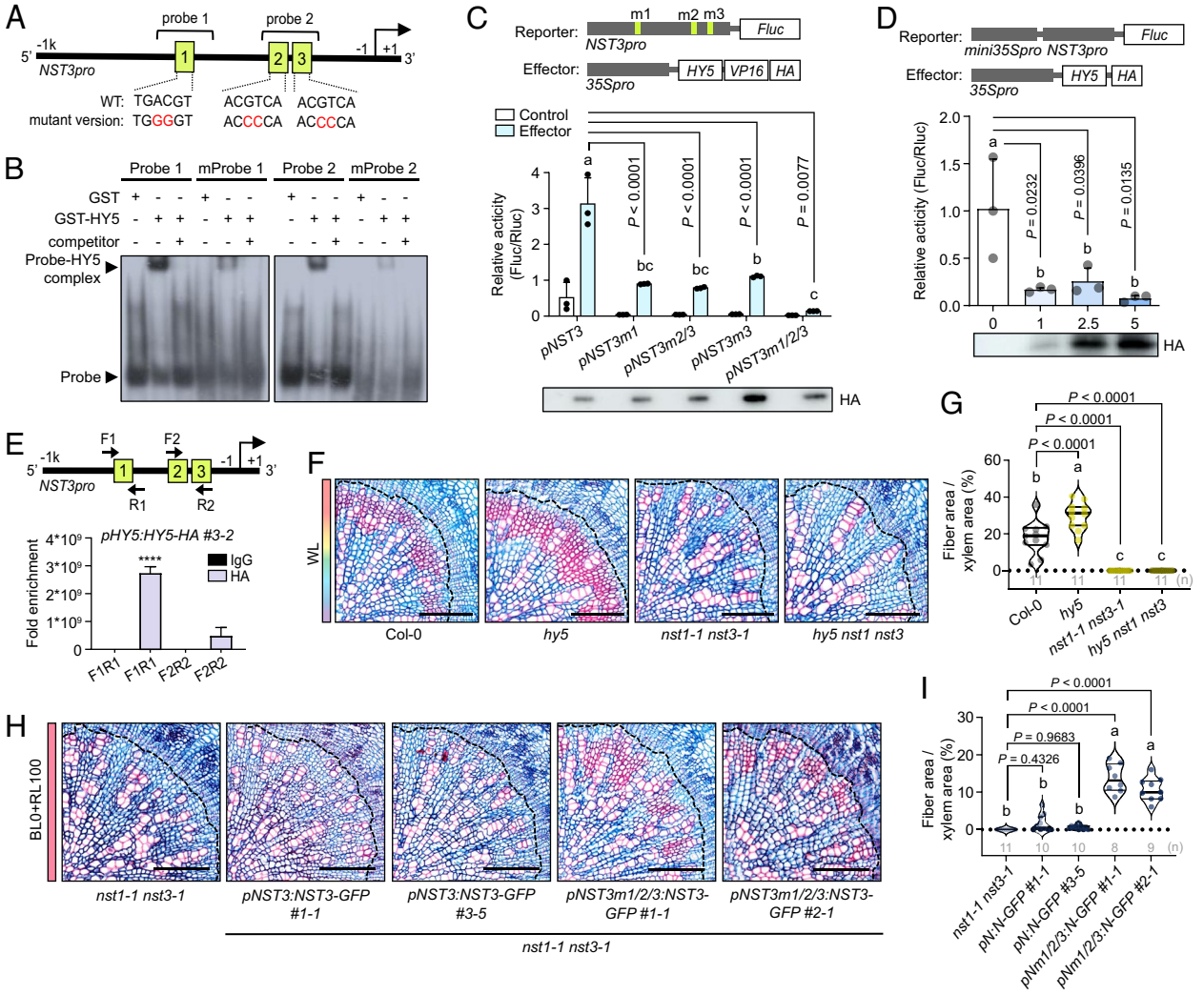

Fig. 5. HY5 directly binds to the *NST3* promoter and suppresses its expression. (*A*) Schematic diagram of putative HY5-binding motifs in the *NST3* promoter, probe design, and mutagenesis for EMSA and reporter analysis. (*B*) EMSA of *NST3* promoter segments (Probes 1 and 2) and its mutants (mProbes 1 and 2) with recombinant GST-HY5. Nonlabeled probes were used as competitors in 100-fold excess relative to radiolabeled probes. GST was used as a negative control. (*C*) Reporter assay using the *NST3* promoter driving the *Fluc* reporter gene and its mutants (*pNST3m*) with or without the effector. Fluc activities were normalized to *UBQ10* promoter-driven Renilla luciferase (*Rluc*). HY5-VP16 protein levels were determined with an anti-HA antibody. (*D*) Reporter assay using minimal-*35S* promoter fused-*NST3* promoter driving the Fluc reporter. LUC activities were normalized to Rluc. Data are means ± SEM (one-way ANOVA followed by Tukey's test). HY5-HA protein levels were determined by probing with an anti-HA antibody. (*E*) CUT&RUN assay of HY5 binding to the *NST3* promoter in *pHY5:HY5-HA* seedlings. An HA antibody was used for the recruitment of pAG-MNase to the HY5 binding site; anti-IgG antibody served as the negative control. (*F*) Hypocotyl cross-sections of Col-0, *hy5*, *nst1-1 nst3-1*, and *hy5 nst1 nst3*. (*G*) Xylem fiber area to xylem area in Col-0, *hy5*, *nst1-1 nst3-1*, and *hy5 nst1 nst3*. Data are means ± SEM ($n \geq 9$; one-way ANOVA followed by Tukey's test). (*H*) Cross-sections of hypocotyls in the *nst1-1 nst3-1* background harboring transgenes consisting of *NST3* driven by *pNST3* or *pNST3m*. (*I*) Xylem fiber area to total xylem area of *pNST3:NST3-GFP* and *pNST3m:NST3-GFP* transgenic plants in the *nst1-1 nst3-1* background. Data are means ± SEM ($n \geq 9$; one-way ANOVA followed by Tukey's test). (Scale bar, 100 μm.)

(*SI Appendix*, Fig. S21 *C–E*). Notably, under blue light conditions at internode 11, where xylem precursor cell expansion is observed, master regulators of these processes were significantly up-regulated, including *NST* homologs (*PtrVNS11* and *PtrVNS12*) (57), and *PtrPAL1* (58), which is involved in the lignin catabolic process (*SI Appendix*, Fig. S21*C*). In internode 10, we also observed a significant increase in the expression of genes downstream of these master regulators, suggesting that blue light activates hierarchical transcriptional reprogramming to promote SCW thickening in libriform fibers, similar to *Arabidopsis* (*SI Appendix*, Fig. S21*D*). At internode 9, following the onset of SCW accumulation, the number of genes exhibiting significant changes in expression decreased (*SI Appendix*, Fig. S21*E*), implying that blue light primarily acts as a signal to trigger the differentiation of libriform fibers within initial vascular tissues of the shoot apex (internode 10 and 11). Additionally, our findings indicate that blue light not only enhances the differentiation of xylem fibers but also significantly contributes to the thickening of the SCW and the elongation of xylem fiber cells (*SI Appendix*, Fig. S21 *F–H*). Overall, these results suggest that the mechanisms of xylem fiber (including libriform fiber) differentiation, which is induced by blue light, might also function in wood formation in trees. Indeed, the recent observation that PtrCRY1 enhances wood formation is likely to relate to a process involving spatiotemporally coordinated light signaling, presumably through PtrHY5 (56, 59).

Discussion

The pursuit of light has been an important driving force in the evolution of land plants, leading to elaborate signaling networks integrating light information (quality and quantity) into plant growth and development. In this study, we revealed that light itself acts as a key signaling cue for the formation of xylem fiber cells, a major component of woody tissue. We identified an

HY5-mediated light signaling pathway that channels light signals from the shoot to the hypocotyl during secondary growth. Importantly, this mechanism functions independently of the direct, local effects of light on hypocotyl elongation observed during photomorphogenesis (19, 54). Therefore, HY5 plays dual roles as a positive regulator of primary growth and as a suppressor of secondary growth. During xylem fiber differentiation, blue light perceived by the shoot steers NST3-dependent xylem fiber formation by impeding the translocation of HY5 from the shoot to the hypocotyl, which occurs due to the nuclear sequestration of HY5 by CRYs in the shoot. It may be through this mechanism that CRYs induce the photoresponse, as described previously (45, 56). The long-distance blue light-CRYs-HY5 module might primarily function at the shoot apex, especially in plants that dominate the canopy over neighboring plants, in environments where blue light predominates (*SI Appendix*, Fig. S21*I*). Hence, a strategy regulating secondary growth might have evolved in trees that use the blue light present above the canopy as a triggering signal to ensure the availability of SCW building blocks.

Trees in boreal and temperate regions adjust their growth patterns to align with the seasonal changes in climate, an adaptation critical for their survival. Plants must sense light at the tip of the shoot, since dormancy and bud break during seasonal growth take place within the shoot apex (60). Our findings demonstrate that blue light serves as a trigger fostering the differentiation of xylem fibers at the shoot apex (Figs. 1*E* and 2 *K* and *L* and *SI Appendix*, Fig. S21 *B*–*E*). This supports the notion that the light spectrum reaching the shoot apex may regulate xylem fiber development via long-distance signal-transduction processes, thereby contributing to the formation of seasonal tree rings. Therefore, plants have likely developed mechanisms to perceive the light environment to ensure secondary growth via an adaptive strategy that utilizes the blue light above the canopy.

Recent studies have suggested a molecular link between light signaling and early vascular tissue development. Single-cell transcriptome analysis showed that exposing etiolated seedlings to light suppresses protoxylem differentiation (51), supporting our finding that light suppresses SCW deposition triggered by CRY-dependent blue light signaling in seedlings (50) (*SI Appendix*, Fig. S11*L*). However, prolonged exposure to light induces differentiation of the protoxylem, which is enhanced by blue light through the CRY1-PIF4-CLE44 signaling module, enabling the transport of water for photosynthesis (42). These findings suggest that light plays a critical role in regulating plant development, as evidenced by its influence on protoxylem differentiation during primary growth and xylem fiber formation during secondary growth. These processes highlight the importance of light in the stage-and tissue-specific regulation of SCW accumulation. However, to fully understand the role of blue light signaling in secondary growth, it is essential to investigate the potential long-distance interactions between the CRYs-HY5-NST3 and local CRY1-MYC2/4-NST1 modules during SCW accumulation in xylem fibers (45) of adult hypocotyls.

At the molecular level, HY5, a master integrator of light signaling, prevents SCW biosynthesis by directly suppressing *NST3* transcription during secondary growth (Figs. 3 and 5), but this mechanism serves as a part of CRY-mediated xylem fiber development (Fig. 4 *G* and *H*). Hence, the existence of a key mechanism promoting xylem fiber formation whereby HY5 operates as a long-distance signal under the control of blue light and CRYs remains an open question, and these long-range factors might be tightly regulated in a spatiotemporal manner by light signaling components. Moreover, long-distance transport of HY5 from the shoot, but not local HY5 activation (Fig. 4*B*), plays an essential role in inhibiting xylem fiber formation (Fig. 5). The specific phosphorylation of HY5 by SPA1 in the shoot (61) might contribute to the transcriptional repressor activity of HY5 on the *NST3* promoter or HY5 protein complex assembly during secondary growth or vice versa. Further detailed biochemical analysis of the tissue-specific posttranslational modification of HY5 should help reveal the spatiotemporal functions of HY5-mediated developmental regulation and its interaction with environmental conditions.

In parallel with the tight control of HY5 protein abundance by COP1/SPA E3 ligase activity, the blue light–dependent nuclear import of CRYs and their complex formation with COP1/SPA and their target HY5 contributes to the retention of HY5 in the nucleus. Blue light–regulated HY5 in cotyledons and hypocotyls acts as a photomorphogenic transcriptional regulator during de-etiolation. After early seedling establishment, the long-term attenuation of the translocation of HY5 to the hypocotyl via CRYs-COP1/SPA in the shoot acts as a signal for xylem fibers during secondary growth (*SI Appendix*, Fig. S21*I*). Although our study focused on secondary growth in the adult hypocotyl, whereas Gao et al. (21) examined primary growth in root tips under phosphate-deficient conditions, both studies highlight the pivotal role of blue light in regulating HY5 mobility. The differences in HY5 translocation in response to blue light in this study versus that of Gao et al. (21) might be due to differences in developmental stages, tissue types, nutrient and growth conditions, and light regimes. These findings highlight the complexity of HY5-mediated signaling and emphasize the need for further study to elucidate the specific environmental and endogenous factors that govern HY5 mobility across different physiological contexts. In addition, we observed HY5 accumulation in vascular cell files of adult leaves and in xylem parenchyma and phloem of adult hypocotyls, suggesting that the HY5-mediated light signaling pathway is adjusted to different cell types through the dynamic switching of interacting transcriptional regulators such as BBX proteins or DELLA (62). This notion clearly aligns with previous reports on the role of HY5 as an activator during primary growth (19, 54) and a repressor during secondary growth. Thus, spatial and temporal analysis of HY5-interacting proteins in specific developmental contexts will improve our understanding of how plants integrate light signals into developmental programs.

Here, we uncovered a genetic network governing blue light–mediated development during secondary growth, particularly xylem fiber production, in *Arabidopsis* hypocotyls and hybrid poplar. However, functional genetic studies on light-controlled wood formation in tree species are needed in order to apply our findings to enhance wood biomass. For instance, an investigation of the conserved action of HY5 in xylem fiber formation in woody plants via CRY-mediated blue light signaling, along with genetic and environmental manipulation, should provide powerful strategies to increase carbon sequestration in wood, which represents a substantial carbon sink in the Earth's ecosystem.

Materials and Methods

Histological Analysis. The hypocotyls of soil-grown 30 DAG or 37 DAG *Arabidopsis* plants or 7-wk-old poplar plants were fixed in 3% formaldehyde and 2.5% glutaraldehyde in 0.1 M phosphate buffer (pH 7.1). The fixed samples were dehydrated in an ethanol series and immersed in Histo-Clear II (National Diagnostics, cat. no. NAT1334). The cleared samples were embedded in Paraplast (Leica, Wetzlar, Germany, cat. no. 39601006), cut into 10 μm sections using a microtome (Leica, Wetzlar, Germany, cat. 149MULTI0C1), and counterstained with 1% Safranin-O (Sigma, cat. no. S2255) and 0.5% Astra blue (Santa-Cruz

Biotechnology, cat. no. sc-214558A). The sections were analyzed using a multi-slide scanner (Olympus, Japan, VS200).

See *SI Appendix* for full details of Methods.

Data, Materials, and Software Availability. The RNA-seq data were deposited in NCBI SRA under accession number PRJNA935048 (49). All other data are included in the manuscript and/or supporting information.

ACKNOWLEDGMENTS. We thank Jeong-il Kim (Chonnam National University) for sharing *bic1 bic2*, *cry1 cry2 GFP-CRY2-OX*, *hy5 HY5-GFP-OX*, and *hy5-ks50*, *hyh*, and *hy5-ks50 hyh* plant materials in the Ws-2 background. This work was supported by a National Research Foundation of Korea (NRF) grant funded by the Korean government (NRF-RS-2023-00209134) to H. Cho.

Author affiliations: [a]Department of Industrial Plant Science and Technology, Chungbuk National University, Cheongju 28644, Korea; [b]Department of Horticultural Science, Chungbuk National University, Cheongju 28644, Korea; [c]Department of Forest Bioresources, National Institute of Forest Science, Suwon 16631, Korea; [d]Department of Biological Sciences, Chungnam National University, Daejeon 34134, Korea; and [e]Department of Agricultural Biotechnology, Seoul National University, Seoul 08826, Korea

1. M. Chen, J. Chory, C. Fankhauser, Light signal transduction in higher plants. *Annu. Rev. Genet.* **38**, 87–117 (2004).
2. E. Bruggemann, K. Handwerger, C. Essex, G. Storz, Analysis of fast neutron-generated mutants at the Arabidopsis thaliana HY4 locus. *Plant J.* **10**, 755–760 (1996).
3. J. Chory, A genetic model for light-regulated seedling Arabidopsis. *Development* **115**, 337–354 (1992).
4. X.-W. Deng, T. Caspar, P. H. Quail, cop1: A regulatory locus involved in light-controlled development and gene expression in Arabidopsis. *Genes Dev.* **5**, 1172–1182 (1991).
5. T. Kinoshita, N. Suetsugu, T. Kagawa, M. Wada, K.-I. Shimazaki, Phot1 and phot2 mediate blue light regulation of stomatal opening. *Nature* **414**, 656–660 (2001).
6. D. J. Kliebenstein, J. E. Lim, L. G. Landry, R. L. Last, Arabidopsis UVR8 regulates ultraviolet-B signal transduction and tolerance and contains sequence similarity to human regulator of chromatin condensation 1. *Plant Physiol.* **130**, 234–243 (2002).
7. B. M. Parks, P. H. Quail, hy8, a new class of arabidopsis long hypocotyl mutants deficient in functional phytochrome A. *Plant Cell* **5**, 39–48 (1993).
8. T. Sakai *et al.*, Arabidopsis nph1 and npl1: Blue light receptors that mediate both phototropism and chloroplast relocation. *Proc. Natl. Acad. Sci. U.S.A.* **98**, 6969–6974 (2001).
9. D. Wagner, J. M. Tepperman, P. H. Quail, Overexpression of phytochrome B induces a short hypocotyl phenotype in transgenic Arabidopsis. *Plant Cell* **3**, 1275–1288 (1991).
10. Y. He *et al.*, Aschoff's rule on circadian rhythms orchestrated by blue light sensor CRY2 and clock component PRR9. *Nat. Commun.* **13**, 5869 (2022).
11. B. Jiang *et al.*, Light-induced LLPS of the CRY2/SPA1/FIO1 complex regulating mRNA methylation and chlorophyll homeostasis in Arabidopsis. *Nat. Plants* **9**, 2042–2058 (2023).
12. X. Wang *et al.*, A photoregulatory mechanism of the circadian clock in Arabidopsis. *Nat. Plants* **7**, 1397–1408 (2021).
13. X. Han, X. Huang, X. W. Deng, The photomorphogenic central repressor COP1: Conservation and functional diversification during evolution. *Plant Commun.* **1**, 100044 (2020).
14. M. T. Osterlund, C. S. Hardtke, N. Wei, X. W. Deng, Targeted destabilization of HY5 during light-regulated development of Arabidopsis. *Nature* **405**, 462–466 (2000).
15. S. N. Gangappa, J. F. Botto, The multifaceted roles of HY5 in plant growth and development. *Mol. Plant* **9**, 1353–1365 (2016).
16. Y. Liu, S. K. Singh, S. Pattanaik, H. Wang, L. Yuan, Light regulation of the biosynthesis of phenolics, terpenoids, and alkaloids in plants. *Commun. Biol.* **6**, 1055 (2023).
17. Y. Xiao *et al.*, HY5: A pivotal regulator of light-dependent development in higher plants. *Front. Plant Sci.* **12**, 800989 (2022).
18. T. Oyama, Y. Shimura, K. Okada, The Arabidopsis HY5 gene encodes a bZIP protein that regulates stimulus-induced development of root and hypocotyl. *Genes Dev.* **11**, 2983–2995 (1997).
19. Y. Burko, C. Gaillochet, A. Seluzicki, J. Chory, W. Busch, Local HY5 activity mediates hypocotyl growth and shoot-to-root communication. *Plant Commun.* **1**, 100078 (2020).
20. X. Chen *et al.*, Shoot-to-root mobile transcription factor HY5 coordinates plant carbon and nitrogen acquisition. *Curr. Biol.* **26**, 640–646 (2016).
21. Y.-Q. Gao *et al.*, Long-distance blue light signalling regulates phosphate deficiency-induced primary root growth inhibition. *Mol. Plant* **14**, 1539–1553 (2021).
22. H.-J. Lee *et al.*, Stem-piped light activates phytochrome B to trigger light responses in Arabidopsis thaliana roots. *Sci. Signal.* **9**, ra106 (2016).
23. K. van Gelderen *et al.*, Far-red light detection in the shoot regulates lateral root development through the HY5 transcription factor. *Plant Cell* **30**, 101–116 (2018).
24. T. Wang *et al.*, Light-induced mobile factors from shoots regulate rhizobium-triggered soybean root nodulation. *Science* **374**, 65–71 (2021).
25. J. Li, J. Zeng, Z. Tian, Z. Zhao, Root-specific photoreception directs early root development by HY5-regulated ROS balance. *Proc. Natl. Acad. Sci. U.S.A.* **121**, e2313092121 (2024).
26. N. D. Bonawitz, C. Chapple, The genetics of lignin biosynthesis: Connecting genotype to phenotype. *Annu. Rev. Genet.* **44**, 337–363 (2010).
27. S. Turner, P. Gallois, D. Brown, Tracheary element differentiation. *Annu. Rev. Plant Biol.* **58**, 407–433 (2007).
28. M. Taylor-Teeples *et al.*, An Arabidopsis gene regulatory network for secondary cell wall synthesis. *Nature* **517**, 571–575 (2015).
29. R. Zhong, T. Demura, Z.-H. Ye, SND1, a NAC domain transcription factor, is a key regulator of secondary wall synthesis in fibers of Arabidopsis. *Plant Cell* **18**, 3158–3170 (2006).
30. M. Kubo *et al.*, Transcription switches for protoxylem and metaxylem vessel formation. *Genes Dev.* **19**, 1855–1860 (2005).
31. N. Mitsuda *et al.*, NAC transcription factors, NST1 and NST3, are key regulators of the formation of secondary walls in woody tissues of Arabidopsis. *Plant Cell* **19**, 270–280 (2007).
32. R. Zhong, E. A. Richardson, Z.-H. Ye, The MYB46 transcription factor is a direct target of SND1 and regulates secondary wall biosynthesis in Arabidopsis. *Plant Cell* **19**, 2776–2792 (2007).
33. R. L. McCarthy, R. Zhong, Z.-H. Ye, MYB83 is a direct target of SND1 and acts redundantly with MYB46 in the regulation of secondary cell wall biosynthesis in Arabidopsis. *Plant Cell Physiol.* **50**, 1950–1964 (2009).
34. W. Li *et al.*, Woody plant cell walls: Fundamental and utilization. *Mol. Plant* **17**, 112–140 (2024).
35. R. Sibout, S. Plantegenet, C. S. Hardtke, Flowering as a condition for xylem expansion in Arabidopsis hypocotyl and root. *Curr. Biol.* **18**, 458–463 (2008).
36. L. Ragni *et al.*, Mobile gibberellin directly stimulates Arabidopsis hypocotyl xylem expansion. *Plant Cell* **23**, 1322–1336 (2011).
37. N. Chaffey, E. Cholewa, S. Regan, B. Sundberg, Secondary xylem development in Arabidopsis: A model for wood formation. *Plant Physiol.* **114**, 594–600 (2002).
38. S. Escamez *et al.*, Fluorescence lifetime imaging as an in situ and label-free readout for the chemical composition of lignin. *ACS Sustain. Chem. Eng.* **9**, 17381–17392 (2021).
39. K. Fukushima, N. Terashima, Heterogeneity in formation of lignin. XIII. Formation of p-hydroxyphenyl lignin in various hardwoods visualized by microautoradiography. *J. Wood Chem. Technol.* **10**, 413–433 (1990).
40. F. Baldacci-Cresp *et al.*, A rapid and quantitative safranin-based fluorescent microscopy method to evaluate cell wall lignification. *Plant J.* **102**, 1074–1089 (2020).
41. C. Chiang, J. E. Olsen, D. Basler, D. Bånkestad, G. Hoch, Latitude and weather influences on sun light quality and the relationship to tree growth. *Forests* **10**, 610 (2019).
42. S. Ghosh, J. F. Nelson, G. M. Cobb, J. P. Etchells, M. de Lucas, Light regulates xylem cell differentiation via PIF in Arabidopsis. *Cell Rep.* **40**, 111075 (2022).
43. T. Mockler *et al.*, Regulation of photoperiodic flowering by Arabidopsis photoreceptors. *Proc. Natl. Acad. Sci. U.S.A.* **100**, 2140–2145 (2003).
44. S. Balasubramanian, S. Sureshkumar, J. Lempe, D. Weigel, Potent induction of Arabidopsis thaliana flowering by elevated growth temperature. *PLoS Genet.* **2**, e106 (2006).
45. Q. Zhang *et al.*, Blue light regulates secondary cell wall thickening via MYC2/MYC4 activation of the NST1-directed transcriptional network in Arabidopsis. *Plant Cell* **30**, 2512–2528 (2018).
46. Q. Wang *et al.*, Photoactivation and inactivation of Arabidopsis cryptochrome 2. *Science* **354**, 343–347 (2016).
47. A.-K. Schürholz *et al.*, A comprehensive toolkit for inducible, cell type-specific gene expression in Arabidopsis. *Plant Physiol.* **178**, 40–53 (2018).
48. P. Hunziker, T. Greb, Stem cells and differentiation in vascular tissues. *Annu. Rev. Plant Biol.* **75**, 399–425 (2024).
49. H. Hwang *et al.*, Transcriptome analysis of hypocotyl in *Arabidopsis thaliana*. NCBI. https://www.ncbi.nlm.nih.gov/bioproject/?term=PRJNA935048. Deposited 15 February 2023.
50. Z. Zhao *et al.*, CRY2 interacts with CIS1 to regulate thermosensory flowering via FLM alternative splicing. *Nat. Commun.* **13**, 7045 (2022).
51. X. Han *et al.*, Time series single-cell transcriptional atlases reveal cell fate differentiation driven by light in Arabidopsis seedlings. *Nat. Plants* **9**, 2095–2109 (2023).
52. T. L. Bailey, J. Johnson, C. E. Grant, W. S. Noble, The MEME suite. *Nucleic Acids Res.* **43**, W39–W49 (2015).
53. M. Holm, L.-G. Ma, L.-J. Qu, X.-W. Deng, Two interacting bZIP proteins are direct targets of COP1-mediated control of light-dependent gene expression in Arabidopsis. *Genes Dev.* **16**, 1247–1259 (2002).
54. Y. Burko *et al.*, Chimeric activators and repressors define HY5 activity and reveal a light-regulated feedback mechanism. *Plant Cell* **32**, 967–983 (2020).
55. Y. Zhang *et al.*, Dissection of HY5/HYH expression in Arabidopsis reveals a root-autonomous HY5-mediated photomorphogenic pathway. *PLoS One* **12**, e0180449 (2017).
56. X. Chen *et al.*, Blue light photoreceptor cryptochrome 1 promotes wood formation and anthocyanin biosynthesis in Populus. *Plant Cell Environ.* **47**, 2044–2057 (2024).
57. M. Ohtani *et al.*, A NAC domain protein family contributing to the regulation of wood formation in poplar. *Plant J.* **67**, 499–512 (2011).
58. J. Yu *et al.*, A PtrLBD39-mediated transcriptional network regulates tension wood formation in Populus trichocarpa. *Plant Commun.* **3**, 100250 (2022).
59. Y. Gao *et al.*, ELONGATED HYPOCOTYL 5a modulates FLOWERING LOCUS T2 and gibberellin levels to control dormancy and bud break in poplar. *Plant Cell* **36**, 1963–1984 (2024).
60. R. K. Singh, T. Svystun, B. AlDahmash, A. M. Jönsson, R. P. Bhalerao, Photoperiod-and temperature-mediated control of phenology in trees–A molecular perspective. *New Phytol.* **213**, 511–524 (2017).
61. W. Wang *et al.*, Direct phosphorylation of HY5 by SPA kinases to regulate photomorphogenesis in Arabidopsis. *New Phytol.* **230**, 2311–2326 (2021).
62. Y. Huang *et al.*, BBX24 interacts with DELLA to regulate UV-B-induced photomorphogenesis in Arabidopsis thaliana. *Int. J. Mol. Sci.* **23**, 7386 (2022).